Chinese Medical Journal®

Single-cell transcriptomics reveals the landscape of immune phenotypes in pituitary neuroendocrine tumors

Zhe Zhang[1,2], Hong Su[3], Jie Yin[1,4], Junhua He[1,5], Yanan Hu[1,2], Peng Li[6], Pinan Liu[1,2]

[1]Department of Neurosurgery, Beijing Tiantan Hospital, Capital Medical University, Beijing 100070, China;
[2]China National Clinical Research Center for Neurological Diseases, Beijing 100070, China;
[3]Cell Biotechnology Laboratory, Tianjin Cancer Hospital Airport Hospital, Tianjin 300000, China;
[4]Department of Neurosurgery, Xuzhou Central Hospital, Xuzhou, Jiangsu 221000, China;
[5]Department of Neurosurgery, Tongde Hospital of Zhejiang Province, Hangzhou, Zhejiang 310012, China;
[6]Department of Neural Reconstruction, Beijing Neurosurgery Institute, Beijing 100070, China.

Abstract

Background: Immune cells critically influence pituitary neuroendocrine tumor (PitNET) progression and therapeutic responses. However, their composition and functional dynamics remain unclear. This study aimed to delineate the immune heterogeneity and intercellular communication networks within PitNETs.

Methods: This study conducted single-cell RNA sequencing (scRNA-seq) on 22 fresh PitNET samples obtained from surgical patients at Beijing Tiantan Hospital between September 2023 and January 2024, with classification based on the expression of key transcription factors: pituitary-specific transcription factor 1 (PIT1), steroidogenic factor 1 (SF1), and T-box transcription factor 19 (TPIT). Following cell type identification, cell–cell communication analysis revealed specific intercellular interactions, which were validated by multiplex immunohistochemistry (mIHC), flow cytometry, and *in vitro* co-culture assays.

Results: The scRNA-seq analysis revealed significant cellular heterogeneity and a lineage-specific immune landscape, including cancer-associated fibroblasts (CAFs), neutrophils, T cells, natural killer cells, and myeloid cells. Specifically, CAF subset distribution was highly lineage-dependent. Collagen-expressing CAF3 was significantly enriched in the PIT1 lineage compared to both TPIT and SF1 lineages. In contrast, inflammatory CAF5 was predominantly found in the TPIT lineage relative to the PIT1 and SF1 lineages. Furthermore, $CD4^+$ regulatory T (Treg) and T follicular helper (Tfh) cells were significantly enriched in the PIT1 lineage relative to the TPIT and SF1 lineages, as validated by both flow cytometry and mIHC data. Cellular communication analysis revealed notable interactions between Treg/Tfh cells and macrophages/microglia that were mediated by the cytotoxic T-lymphocyte-associated protein 4 (CTLA4)–CD86 pathway. Subsequent mIHC assays confirmed spatial colocalization of Treg cells with macrophages/microglia. Complementing these findings, *in vitro* co-culture assays demonstrated functional CTLA4–CD86 signaling specifically between Treg cells and macrophages, providing deeper insights into the complex cellular crosstalk within the PitNET tumor microenvironment (TME).

Conclusions: The three major PitNET lineages exhibited distinct immune cell frequencies, with the PIT1 lineage notably enriched in Treg and Tfh cells, as well as collagen-producing CAF3. Furthermore, a novel immunosuppressive interaction between Treg cells and macrophages, mediated by the CTLA4–CD86 pathway, was identified, suggesting its potential regulatory role within the TME.

Keywords: Immune cells; Intercellular communication; Pituitary neuroendocrine tumors; Single-cell RNA sequencing; Tumor microenvironment

Introduction

Pituitary neuroendocrine tumors (PitNETs), formerly known as pituitary adenomas, account for a significant proportion of intracranial neoplasms.[1,2] These tumors originate from anterior pituitary cells and are classified according to adenohypophyseal hormones and transcription factors, such as pituitary-specific transcription factor 1 (PIT1), T-box transcription factor 19 (TBX19, also known as TPIT), and steroidogenic factor 1 (SF1).[3] A defining feature of PitNETs is their biological heterogeneity, which manifests in variations in cellular composition, hormone secretion profiles, and growth patterns.[4] Some aggressive subtypes display resistance to conventional therapies, including surgery, medical treatment, and radiotherapy,

Access this article online

Quick Response Code:

Website: www.cmj.org

DOI: 10.1097/CM9.0000000000003918

Correspondence to: Pinan Liu, Department of Neurosurgery, Beijing Tiantan Hospital, Capital Medical University, Beijing 100070, China; China National Clinical Research Center for Neurological Diseases, Beijing 100070, China
E-Mail: pinanliu@ccmu.edu.cn;
Peng Li, Department of Neural Reconstruction, Beijing Neurosurgery Institute, Beijing 100070, China
E-Mail: lipengttyyns@163.com

Copyright © 2026 The Chinese Medical Association, produced by Wolters Kluwer, Inc. under the CC-BY-NC-ND license. This is an open access article distributed under the terms of the Creative Commons Attribution-Non Commercial-No Derivatives License 4.0 (CCBY-NC-ND), where it is permissible to download and share the work provided it is properly cited. The work cannot be changed in any way or used commercially without permission from the journal.

Chinese Medical Journal 2026;139(4)

Received: 27-10-2025; **Online:** 09-01-2026 **Edited by:** Xuehong Zhang

further complicating clinical management.[5] Although many studies have focused on molecular mechanisms to improve therapies, the understanding of the PitNET heterogeneity remains limited.

Emerging evidence highlights that the tumor microenvironment (TME) influences PitNET progression and therapeutic efficacy.[6,7] Recent single-cell transcriptomics studies have characterized the TME in PitNETs, showing significant diversity in tumor-associated macrophages (TAMs) and T lymphocytes across different PitNET lineages.[8–11] Despite these advancements, the functional polarization of $CD4^+$ T helper subsets, which differently regulates antitumor immunity, remains poorly understood. In addition, cancer-associated fibroblasts (CAFs) are a major component of the tumor stroma and serve as essential regulators of tumor maintenance and progression through diverse mechanisms.[12] Critically, the substantial molecular heterogeneity and divergent functional and metabolic profiles across CAF subsets demand systematic investigation.

Immune checkpoint inhibitors (ICIs) targeting key inhibitory receptors, including lymphocyte activation gene 3 (LAG3), cytotoxic T-lymphocyte-associated protein 4 (CTLA4), and programmed cell death protein 1 (PD1), enhance antitumor immunity by alleviating T-cell suppression.[13] However, their clinical efficacy remains limited in aggressive PitNETs, with only approximately one-third of patients achieving objective responses.[14] This limited efficacy is influenced by a variety of factors, including the quality and magnitude of tumor-infiltrating lymphocytes,[15] heterogeneous expression of immune checkpoints, such as programmed death-ligand 1 (PD-L1) across PitNET subtypes,[16] and TAM-mediated immunosuppression within the TME.[17] Moreover, the composition, spatial distribution, and interactions of tumor-infiltrating immune cells may also significantly impact clinical outcomes.[18–20] Nevertheless, the fundamental mechanisms of limited efficacy in PitNETs remain incompletely understood. This study aimed to delineate the immune heterogeneity and intercellular communication networks within PitNETs to provide novel insights for advancing PitNET immunotherapies.

Methods

Clinical samples

A total of 22 fresh PitNET samples were collected from patients undergoing surgical resection at Beijing Tiantan Hospital from September 2023 to January 2024. All patients were subsequently diagnosed with PitNET according to the current World Health Organization (WHO) classification of pituitary tumors.[3] Clinical characteristics, including age, sex, and Knosp grade classification,[21] were extracted from electronic medical records [Supplementary Table 1, http://links.lww.com/CM9/C703]. This study was approved by the Institutional Review Board of Beijing Tiantan Hospital (No. KY2023-170-02). Written informed consent was obtained from all participants.

Single-cell RNA sequencing (scRNA-seq) and data analysis

After fresh tumor samples were processed into cell suspension at a concentration of 1×10^5 cells/mL, scRNA-seq was performed using a microfluidic chip and the Illumina (San Diego, CA, USA) HiSeq X10 platform.[22] The raw scRNA-seq datasets were processed using CellRanger-7.0.0 (Pleasanton, California, USA), and the Genome Reference Consortium Human Build 38 (GRCh38) was used as the reference genome. Then, quality control was performed at the single-cell level. Cells were removed if they had fewer than 200 genes or more than 10% mitochondrial genes, and potential doublets were identified using DoubletFinder (v2.0.3, https://github.com/chris-mcginnis-ucsf/DoubletFinder).[23] Subsequently, general single-cell data analyses were performed, including normalization, batch effect correction, and clustering. Furthermore, exploratory analyses were conducted, including cell–cell communication,[24] single-cell metabolomics analysis,[25] and pseudotime analysis to infer macrophage developmental trajectories using RNA velocity[26] and Partition-based Graph Abstraction (PAGA) for trajectory directionality.[27] The detailed methods for these analyses are described in the Supplementary Materials, http://links.lww.com/CM9/C703.

Survival analysis and correlation analysis

Survival and pairwise correlation analyses of gene expression signatures were conducted using the GEPIA2 web server (http://gepia2.cancer-pku.cn/).[28] The specific gene sets and subgroups for the lower-grade glioma (LGG) and glioblastoma (GBM) cohorts are detailed in the Supplementary Materials, http://links.lww.com/CM9/C703.

Gene function and signature analysis

Differential gene expression analysis was performed to identify signature genes within each program. To analyze metabolic differences across various subsets, Single-cell Gene Set Variation Analysis (scGSVA),[29] a single-cell implementation of GSVA,[30] was employed. The activity of cell clusters in specific pathways and biological processes was assessed using gene sets derived from the Kyoto Encyclopedia of Genes and Genomes (KEGG) database,[31] Hallmark gene sets,[32] and Gene Ontology (GO).[33] Metascape,[34] an online platform for experimental biologists, provides comprehensive gene list annotation and analysis. Using this tool, we carried out an in-depth investigation of the biological processes associated with each neutrophil cluster, focusing on the top 100 differently expressed genes.

Flow cytometry

For surface phenotype analysis, the single-cell suspension was stained with the following panel of surface antibodies: CD3 (No. 566779, BD Biosciences, San Jose, CA, USA), CD4 (No. 980804, BD Biosciences), CD25 (No. M-A251, BioLegend, San Diego, CA, USA), CD44 (No. 60-0441-U100, Tonbo, San Diego, CA, USA), PD1 (No. 561273, BD Biosciences), and C-X-C chemokine receptor

type 5 (CXCR5, No. 356919, BioLegend) antibodies at a concentration of 5 μg/10^6 cells in magnetic activated cell sorting buffer for 30 min, shielded from light at room temperature. For intracellular staining, following fixation and permeabilization (No. 554714, BD Biosciences) for 1 h at 4°C, cells were incubated with forkhead box protein P3 (FOXP3) antibodies (No. MA5-44084, Invitrogen, Carlsbad, CA, USA) in permeabilization buffer for 30 min at 4°C in the dark. Samples were analyzed using a BD LSR Fortessa flow cytometer, and data were processed with FlowJo V10 software (BD Biosciences).

CD86⁺ macrophage co-culture with naive CD4⁺ T cell assay

Naive CD4⁺ T cells were magnetically isolated from healthy donor peripheral blood mononuclear cells using the naive CD4⁺ T cell isolation kit (No. 130-094-131, Miltenyi Biotec, Bergisch Gladbach, Germany). Regulatory T (Treg) cell differentiation was induced using a modified protocol adapted from a previous study.[35] For co-culture experiments, naive CD4⁺ T cells (1 × 10^6 cells/well) were plated in Roswell Park Memorial Institute 1640 (RPMI 1640) complete medium containing 10% fetal bovine serum (FBS) and 1% penicillin-streptomycin across five biological replicates. Specifically, in the co-culture group, CD86⁺ macrophages (1 × 10^5 cells/well) or anti-CD86 antibody (10 μg/mL, No. C2158, Leinco, St. Louis, MO, USA) was added to the wells. After 4 days, cells were collected and simultaneously stained with surface antibodies: anti-CD4 (No. 317416, BioLegend), anti-CD25 (No. 302616, BioLegend), and anti-CD127-BV605 (No. 351328, BioLegend). Data acquisition was performed using an LSR Fortessa flow cytometer and the data were analyzed using FlowJo V10 software.

Multiplex immunohistochemistry (mIHC)

We used the following fluorescently labeled antibodies in the staining procedure: CD68 mouse anti-human antibody (No. GB11315, Servicebio, Hubei, China), periostin (POSTN) rabbit anti-human antibody (No. AB215199, Abcam, Cambridge, MA, USA), CD4 mouse anti-human antibody (No. GB13588, Servicebio), CD3 rabbit anti-human antibody (No. GB12014, Servicebio), FOXP3 rabbit anti-human antibody (No. GB112325, Servicebio), inducible T-cell costimulator (ICOS) mouse anti-human antibody (No. AB224644, Abcam), and 4′,6-diamidino-2-phenylindole (DAPI, No. 422801, BioLegend). We diluted the antibodies and processed the samples according to the manufacturer's instructions. The slides were scanned using 3DHISTECH's (Budapest, Hungary) Slide Converter scanning system (Pannoramic MIDI), and the images were analyzed using the CaseViewer2.3 software (3DHISTECH).

Histological diagnosis

The surgically resected samples were fixed in 10% buffered formalin and subsequently embedded in paraffin for the preparation of pathological sections. Histological diagnoses were made based on hematoxylin and eosin (H&E)-stained sections. IHC staining was conducted to evaluate the expression of three transcription factors (PIT1, SF1, and TPIT) and hormone production markers, including growth hormone, prolactin (PRL), thyroid-stimulating hormone, follicle-stimulating hormone, luteinizing hormone, and adrenocorticotropic hormone (ACTH), to characterize tumor subtypes.[36] Pathological evaluations were conducted by experienced neuropathologists.

Statistical analysis

All statistical analyses were performed using R version 4.2.1 (R Foundation for Statistical Computing, Vienna, Austria). Depending on the data distribution, Wilcoxon rank-sum tests and one-way analysis of variance, with correction for multiple comparisons, were used to compare differences among three or more groups. All reported *P* values were two-sided, and statistical significance was defined as $P < 0.05$. To account for multiple testing, *P* values were adjusted using the Benjamini and Hochberg method to control the false discovery rate.

Results

Single-cell transcriptional landscape of PitNETs

To analyze the tumor-infiltrating immune cells in PitNETs, scRNA-seq was performed on tumor tissues from 22 patients with PitNETs, which included 5 PIT1 tumors, 7 SF1 tumors, 8 TPIT tumors, and 2 tumors with multiple cell lineages (MIX), classified by three transcription factors [Figure 1A and Supplementary Table 1, http://links.lww.com/CM9/C703]. After stringent quality control, a total of 287,051 single cells were selected for further analysis. Then uniform manifold approximation and projection (UMAP) was applied for dimensionality reduction and cell annotation. As a result, 13 distinct cell types were identified within the TME, including epithelial cells, macrophages, neutrophils, microglial cells, neural cells, T cells, natural killer (NK) cells, fibroblasts, dendritic cells (DCs), endothelial cells (ECs), mast cells, B cells, plasmacytoid dendritic cells (pDCs), and plasma cells [Figure 1B–F]. The distribution of epithelial cells, arranged in descending order, corresponded to MIX-, PIT1-, TPIT-, and SF1-lineage PitNETs. In addition, there were higher proportions of macrophages, microglial cells, fibroblasts, ECs, and mast cells in SF1 lineage tumors. In contrast, T and NK cells, DCs, B cells, pDCs, and plasma cells were abundant in PIT1 lineage tumors. Neutrophils were abundant in TPIT lineage tumors [Figure 1D]. These data demonstrated substantial variations in immune cell distribution across different PitNET lineages.

Characterization of epithelial cells in PitNETs

In this study, five epithelial cell types were identified across four PitNET lineages: Tumor cells, stem cells, corticotropes, gonadotropes, and pro-PIT1 cells [Supplementary Figure 1A–E, http://links.lww.com/CM9/C703]. Tumor cells were predominant in all lineages. The PIT1 lineage exhibited a higher proportion of stem cells and pro-PIT1 cells compared to the other lineages, while corticotropes were predominantly localized to the TPIT lineage.

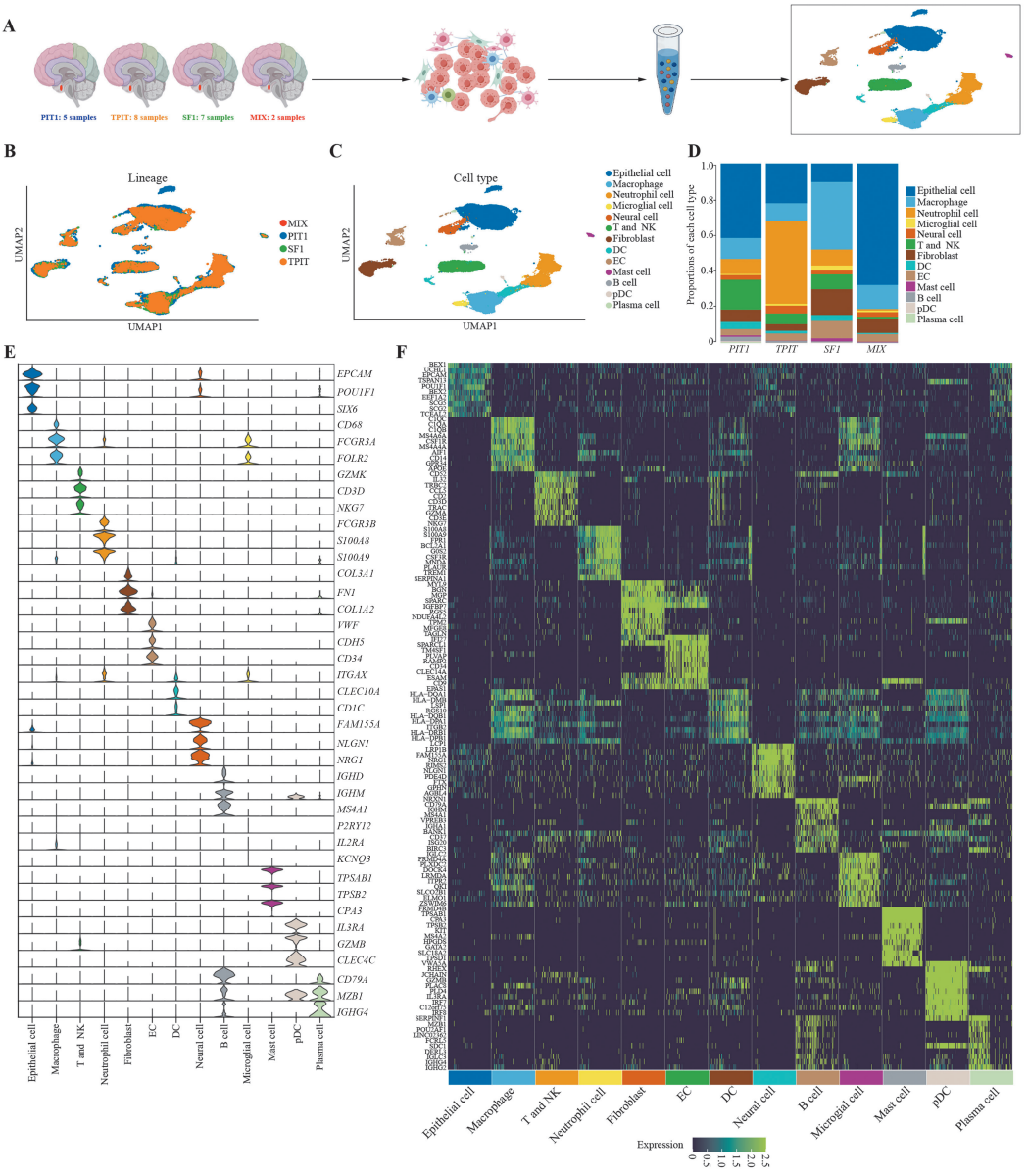

Figure 1: Single-cell transcriptomic atlas of the tumor microenvironment in PitNETs. (A) Overview of the study workflow from sample processing to single-cell data analysis. (B) UMAP visualizes 287,051 single cells from 22 patients with distinct lineage PitNETs, with color-coding indicating their identities. (C) UMAP displays the major cell types in PitNETs, with color-coding identifying their respective identities. (D) Bar graph demonstrates the proportions of each cell type in different PitNET lineages. (E) Violin plot illustrates the expression of marker genes across distinct cell types. (F) Heatmap illustrates the expression level of top differentially expressed genes in each cell type. DC: Dendritic cell; EC: Endothelial cell; MIX: Multiple cell lineages; NK: Natural killer; pDC: Plasmacytoid dendritic cell; PIT1: Pituitary-specific transcription factor 1; PitNETs: Pituitary neuroendocrine tumors; SF1: Steroidogenic factor 1; TPIT: T-box transcription factor 19; UMAP: Uniform manifold approximation and projection.

Gonadotropes showed increased frequencies in SF1 and MIX lineages compared to other groups [Supplementary Figure 1C, http://links.lww.com/CM9/C703]. These findings suggested that distinct epithelial cell types existed across the four PitNET lineages. Copy number variation (CNV) was calculated to assess the malignant status of four epithelial cell types [Supplementary Figure 1F, http://links.lww.com/CM9/C703]. These results revealed that gonadotropes and corticotropes exhibited higher CNV levels compared to other cell types, suggesting a greater malignant potential.

Metabolic differences among the five epithelial cell types were systematically analyzed using scMetabolism. Metabolic pathway activity analysis revealed enrichment of tumor cells in fatty acid metabolism and the citrate cycle, while stem cells were associated with glutathione metabolism, as well as ascorbate and aldarate metabolism pathways. Notably, tumor cells, stem cells, and pro-PIT1 cells all showed associations with oxidative phosphorylation [Supplementary Figure 1G, http://links.lww.com/CM9/C703]. Furthermore, metabolomic activity heterogeneity was observed across all five cell types, with tumor cells and stem cells exhibiting elevated metabolic activity compared to other cell types [Supplementary Figure 1H, http://links.lww.com/CM9/C703]. These findings demonstrated pronounced compositional and metabolomic heterogeneity among the distinct epithelial cell types in PitNETs.

Heterogeneity of CAF in PitNETs

Five CAF subsets were identified across PitNET lineages. Notably, CAF subset proportions varied across lineages, with CAF3 predominant in the PIT1 lineage and CAF5 dominating the TPIT lineage [Figure 2A–C]. CAF3 expressed genes related to collagen, such as *COL1A1*, *POSTN*, and *LUM*, whereas CAF5 expressed inflammatory-associated genes like *CXCL8*, *ATF3*, and *IL6* [Figure 2D]. Further analysis of CAF subset differences revealed that CAF3 exhibited the lowest differentiation status, indicating strong stemness and a high differentiation potential [Figure 2E]. In addition, the biological functions of the CAF3 and CAF5 were characterized. Pathway analysis showed CAF3 enrichment in extracellular matrix (ECM)-related processes, including ECM receptor interaction, protein

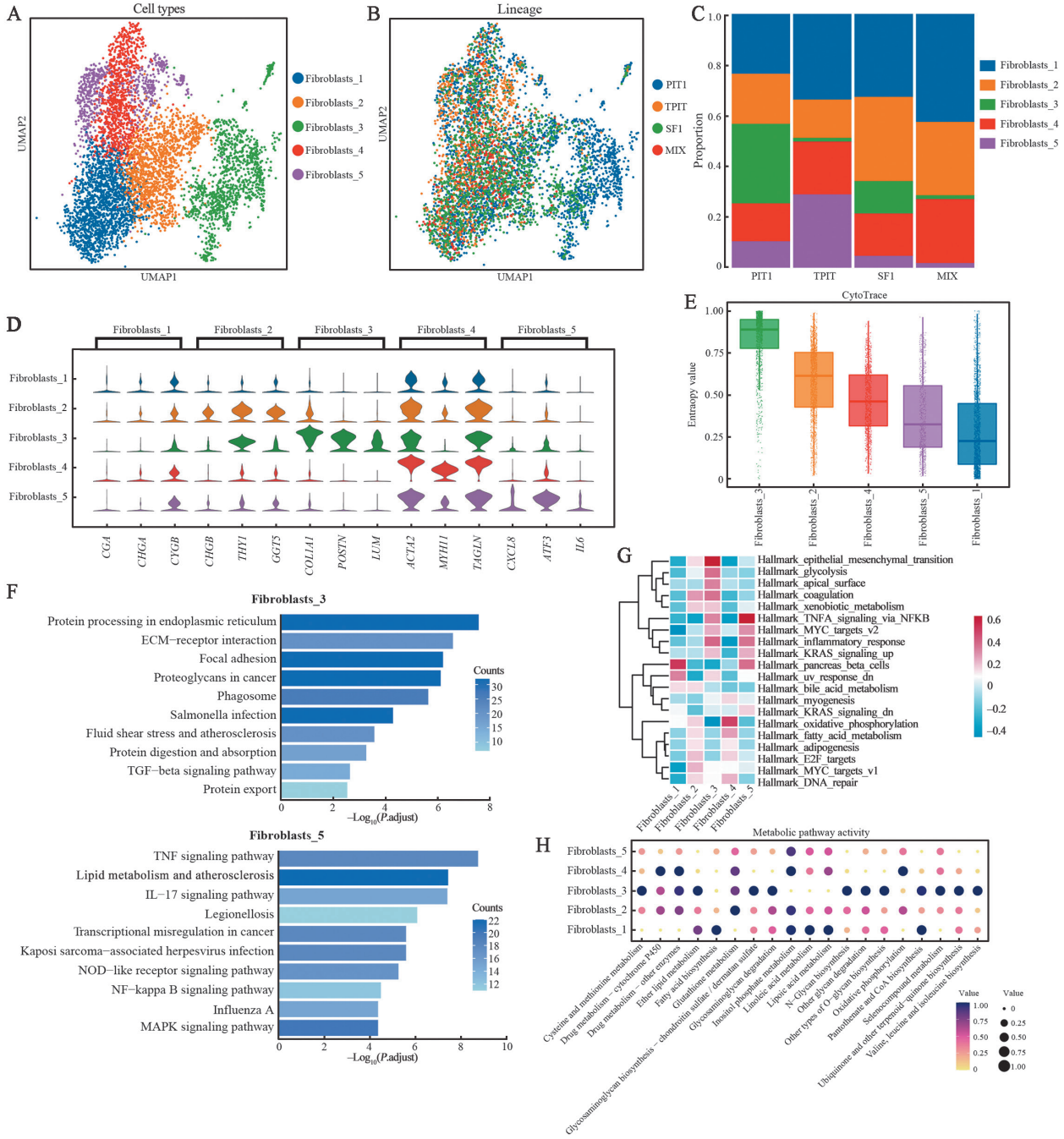

Figure 2: The heterogeneity of CAFs in PitNETs. (A, B) UMAP visualization identifies five CAF subsets (A) and distinct PitNET lineages (B) from single-cell data, with color-coding indicating their identities. (C) Bar graph illustrates the compositional distribution of five CAF subsets in different PitNET lineages. (D) Violin plot showing the expression of top three genes within each CAF subset. (E) CytoTRACE infers the differentiation status of distinct CAF subsets. (F) Bar plot depicting enrichment of upregulated genes in distinct signaling pathways for the CAF3 and CAF5 subsets. (G) Heatmap shows the top differentially enriched pathways across the five distinct CAF subsets, as identified by GSVA. (H) Dot plot shows the metabolic pathway activity of five distinct CAF subsets, using scMetabolism analysis. The circle size and color darkness both represent the scaled metabolic score. CAF: Cancer-associated fibroblast; CoA: Coenzyme A; GSVA: Gene set variation analysis; MIX: Multiple cell lineages; PIT1: Pituitary-specific transcription factor 1; PitNETs: Pituitary neuroendocrine tumors; SF1: Steroidogenic factor 1; TPIT: T-box transcription factor 19; UMAP: Uniform manifold approximation and projection.

processing, and focal adhesion, all of which contribute to creating a TME conducive to tumorigenesis and metastasis [Figure 2F]. Conversely, CAF5 exhibited enrichment in the TNF signaling pathway, lipid metabolism and atherosclerosis, and the IL-17 signaling pathway [Figure 2F]. GSVA analysis of the CAF subset signatures further revealed CAF3 enrichment in epithelial-mesenchymal transition, glycolysis, and apical surface. These processes were crucial for epithelial integrity and function. In contrast, CAF5 was associated with inflammatory responses, TNFα signaling via nuclear factor kappa B (NF-κB), and MYC target pathways. CAF2 and CAF4 were associated with oxidative phosphorylation and fatty acid metabolism [Figure 2G]. Furthermore, scMetabolism analysis demonstrated that CAF3 actively participates in the metabolic pathways of amino acids, glycosaminoglycans, and various other substances [Figure 2H]. The involvement of CAFs in these metabolic pathways suggested a potential susceptibility to endocrine abnormalities.

Identify the characteristic of myeloid cells in PitNETs

Through systematic single-cell analysis, dimensionality reduction-based clustering was applied to the myeloid compartment, excluding neutrophils and mast cells, and identified seven phenotypically distinct mononuclear phagocyte (MP) populations across different PitNET lineages, including proliferating MPs, macrophages, monocytes, conventional dendritic cell type 1 (cDC1), conventional dendritic cell type 2 (cDC2), microglial cells, and pDCs [Figure 3A–C]. Notably, monocytes and DCs (cDC1, cDC2, and pDCs) were predominantly localized in PIT1 lineage tumors. In contrast, the proportion of microglial cells was higher in SF1 and mixed lineages compared to those in other lineages [Figure 3D]. Then, the metabolic activity of these MP populations was investigated within PitNETs. As illustrated in Figure 3E, macrophages and microglial cells displayed elevated metabolic activity. This suggested that macrophages, the predominant immune cells in PitNETs, were susceptible to hormone secretion.

In light of the variable proportions of microglial cells among PitNET lineages, their functional profiles were compared across PIT1, SF1, and TPIT lineages. Differentially expressed genes were visualized using a volcano plot. In contrast to the SF1 lineage, microglial cells in PIT1 and TPIT lineages exhibited higher expression of C-X3-C motif chemokine receptor 1 (CX3CR1) and basic-helix-loop-helix family member e41 (BHLHE41), which were associated with microglial and macrophage responses. Conversely, SF1-lineage microglial cells preferentially expressed chemokine-related genes [Figure 3F–G]. Moreover, microglial cells in the PIT1 and TPIT lineages appear to be involved in neutrophil activation, neutrophil-mediated immunity, neutrophil degranulation, and response to interferon-γ [Figure 3H]. Furthermore, the development of macrophages was thoroughly investigated. Comprehensive data on these immune cells were collected, and RNA velocity was utilized to deduce their developmental pathways. Macrophage-derived cell subsets were identified, including Macrophages_C1QB, Macrophages_ELMO1, Macrophages_FGL2, Macrophages_CXCL3, and Microglial cells_CX3CR1. Macrophages_C1QB serves as a common progenitor cell capable of differentiating into Macrophages_CXCL3 and Microglial cells_CX3CR1 [Figure 3I]. Additionally, an increase in the mRNA levels of interleukin-6 signal transducer (*IL6ST*), NFKB inhibitor alpha (*NFKBIA*), and transformer 2 beta homolog (*TRA2B*) was observed during the development of macrophages into Microglial cells_CX3CR1 [Figure 3J]. This suggested that Microglial cells_CX3CR1, as a terminally differentiated macrophage subset, contributed to PitNET immune responses.

Heterogeneity of neutrophils in PitNETs

Eight transcriptionally distinct neutrophil subsets were identified, showing differential distribution across PitNET lineages [Supplementary Figure 2A–C, http://links.lww.com/CM9/C703]. Among these, the secreted phosphoprotein 1 (SPP1)-expressing subset dominated the PIT1 lineage, while the cathelicidin antimicrobial peptide (CAMP)-expressing subset was mainly enriched in the TPIT lineage [Supplementary Figure 2C–D, http://links.lww.com/CM9/C703]. Furthermore, these eight neutrophil subsets were associated with distinct biological processes. The IL1B, SPP1, CAMP, and S100A12 neutrophil subsets were significantly enriched in regulating leukocyte activation, humoral immune response, and inflammatory response. The neutrophils_ISG15 were highly enriched in antiviral processes, including interferon-stimulated gene antiviral mechanisms, defense against viruses, and responses to type I interferon. The neutrophils_CXCR1 were only enriched in peptide chain elongation processes [Supplementary Figure 2E, http://links.lww.com/CM9/C703].

In addition, additional brain tumor datasets (by combining LGG and GBM into a single cohort) were integrated, and GEPIA2 was used to evaluate the clinical relevance and immune-related functions of neutrophils_SPP1 and neutrophils_CAMP. Notably, patients with high expression of SPP1 [Supplementary Figure 2F, http://links.lww.com/CM9/C703] and CAMP [Supplementary Figure 2H, http://links.lww.com/CM9/C703] showed a significantly reduced overall survival (OS) (P <0.001). The SPP1 subset showed strong correlations with both microglial cells (R = 0.82, P <0.001) and Treg cells (R = 0.81, P <0.001) [Supplementary Figure 2G, http://links.lww.com/CM9/C703]. In contrast, the CAMP subset was strongly correlated with microglial cells (R = 0.83, P <0.001), but exhibited only a moderate correlation with Treg cells (R = 0.44, P <0.001) [Supplementary Figure 2I, http://links.lww.com/CM9/C703]. These findings indicate that specific neutrophil subsets are associated with poor clinical outcomes. Moreover, these neutrophil subsets exhibit functional associations with microglial cells and/or Treg cells.

Diversity of tumor-infiltrating T cells in PitNETs

Our study identified 13 subsets within distinct lineage PitNETs, including proliferating T cells, NaiveT_LTB, NaiveT_SELL, Tfh_PDCD1, NK_XCL2, NK_FCGR3A, Treg_FOXP3, NaiveT_IL7R, NaiveT_TCF7, CD8Teff_CCL4, CD8Teff_GZMA, CD8Teff_KLRB1, and CD8Trm_ZNF683 [Figure 4A and B]. Moreover, $CD4^+$ and $CD8^+$

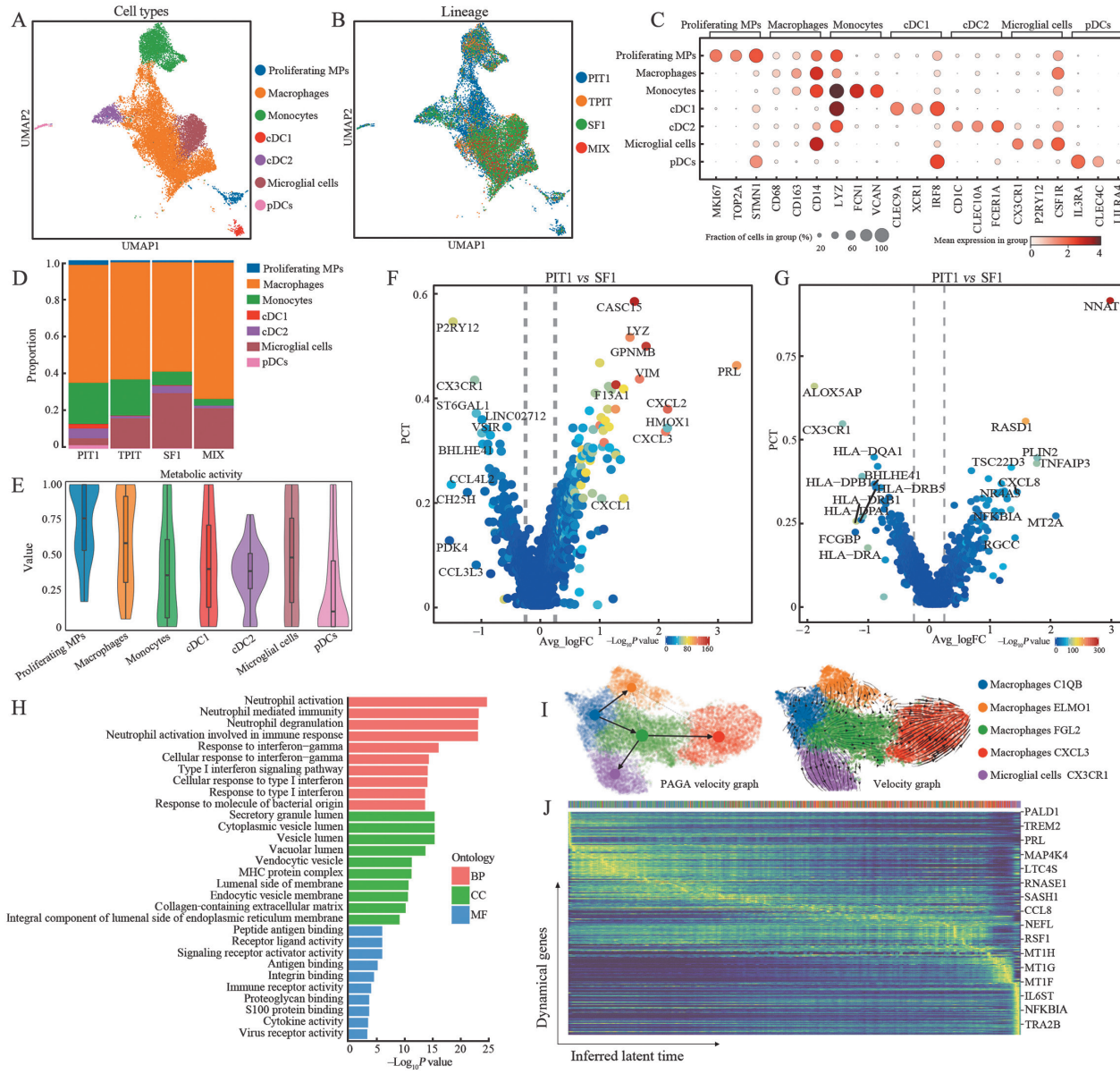

Figure 3: The heterogeneity of MPs in PitNETs. (A, B) UMAP displaying seven MP populations (A) and four PitNET lineages (B), with color-coding indicating their identities. (C) Dot plot displaying the expression of top three genes across cell types. (D) Bar graph depicting the proportional distribution of each cell type across distinct PitNET lineages. (E) Box plot showing the distribution of metabolic activity across different cell types, based on scMetabolism. (F, G) Volcano plots showing the differentially expressed genes of microglial cells across distinct lineages. PIT1 *vs.* SF1 (F) and TPIT *vs.* SF1 (G). (H) For microglial cells, GO enrichment analysis further identifies the signaling pathways enriched among genes upregulated relative to the SF1 lineage. (I) The developmental trajectory analysis of macrophages. In the PAGA velocity graph, solid lines indicate stronger relationships than dashed lines. The velocity graph includes arrows representing the direction of cellular differentiation. (J) Heatmap of top-likelihood genes illustrates dynamic gene expression changes during the development of macrophages into Microglial cells_CX3CR1. BP: Biological process; CC: Cellular component; cDC1: Conventional dendritic cell type 1; cDC2: Conventional dendritic cell type 2; GO: Gene ontology; MF: Molecular function; MHC; Major histocompatibility complex; MIX: Multiple cell lineages; MP: Mononuclear phagocyte; PAGA: Partition-based Graph abstraction; pDC: Plasmacytoid dendritic cell; PIT1: Pituitary-specific transcription factor 1; PitNETs: Pituitary neuroendocrine tumors; SF1: Steroidogenic factor 1; TPIT: T-box transcription factor 19; UMAP: Uniform manifold approximation and projection.

T-cell subsets displayed distinct distribution patterns across PitNET lineages. CD8⁺ effector T cells exhibited complex distribution profiles across different PitNET lineages. Furthermore, CD4⁺ Treg and T follicular helper (Tfh) cells were predominantly enriched in the PIT1 lineage, showing higher abundance compared to the TPIT and SF1 lineages [Figure 4C and D]. Flow cytometric quantification revealed significant variation in Treg and Tfh cell frequencies across PitNET lineages. Notably, PIT1 tumors exhibited elevated proportions of these immunomodulatory cells despite the relatively low abundance of overall CD4⁺ T cell infiltration [Figure 4E, Figure 4F and Supplementary Figure 3, http://links.lww.com/CM9/C703]. In addition, this finding was quantitatively assessed using mIHC, which revealed significantly elevated expression of CD3, CD4, FOXP3, and ICOS in the PIT1 lineage compared to others (P <0.001) [Figure 4G and Supplementary Figure 4, http://links.lww.com/CM9/C703].

T cell molecular signatures were further characterized through scGSVA. Treg cells showed significant enrichment in the bile acid metabolism and interleukin-6/Janus

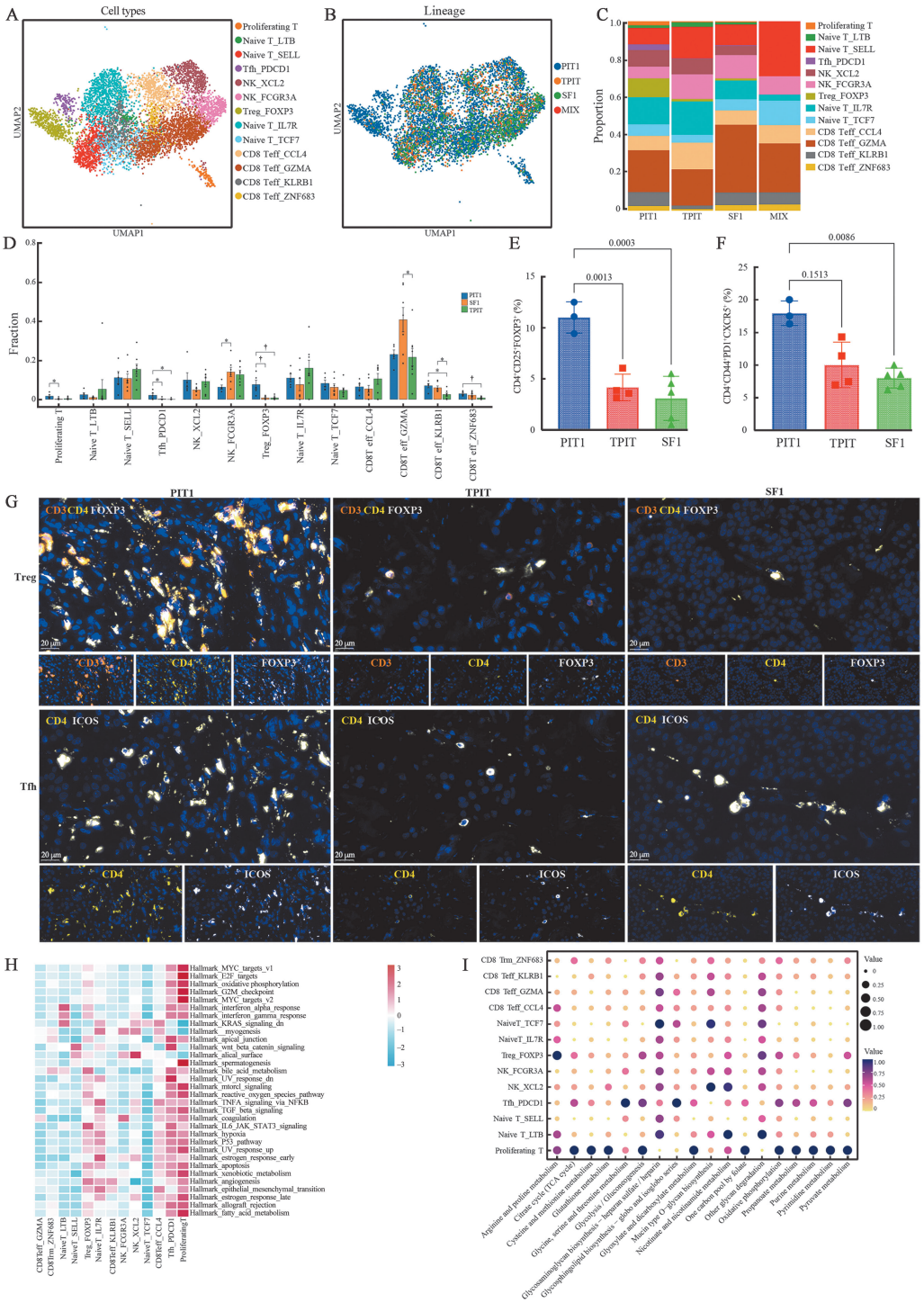

Figure 4: Single-cell profiling of T-cell subsets in PitNETs. (A, B) UMAP visualization of 13 T-cell subsets (A) and four PitNET lineages (B), with color-coding indicating their identities. (C) Bar graph showing the proportions of distinct T-cell subsets across various PitNET lineages. (D) Comparison of distinct T-cell subsets distribution among PIT1, TPIT, and SF1 PitNET lineages. $^{*}P<0.05$; $^{\dagger}P<0.01$. (E, F) Bar graphs indicate the frequencies of Treg and Tfh cells in different lineage tumors (PIT1, $n = 3$; TPIT, $n = 4$; SF1, $n = 5$). (E): $CD4^+$ $CD25^+$ $FOXP3^+$; (F) $CD4^+$ $CD44^+$ $PD1^+$ $CXCR5^+$. (G) Representative mIHC staining displaying the presence of $CD4^+$ $FOXP3^+$ Treg cells (orange, yellow, and white represent Treg cells) and $CD4^+$ $ICOS^+$ Tfh cells (yellow and white represent Tfh cells) in different lineage tumors (PIT1, $n = 3$; TPIT, $n = 3$; SF1, $n = 3$). Scale bar as indicated. (H) scGSVA reveals the hallmark pathways across distinct T-cell subsets. (I) Dot plot showing metabolic pathway activity of defined T-cell subsets, analyzed by scMetabolism. The circle size and color darkness both represent the scaled metabolic score. CD: Cluster of differentiation; CXCR5: C-X-C chemokine receptor type 5; FOXP3: Forkhead box protein P3; ICOS: Inducible T-cell costimulator; mIHC: Multiplex immunohistochemistry; MIX: Multiple cell lineages; PD1: Programmed cell death protein 1; PIT1: Pituitary-specific transcription factor 1; PitNETs: Pituitary neuroendocrine tumors; scGSVA: Single-cell gene set variation analysis; SF1: Steroidogenic factor 1; Tfh: T follicular helper; TPIT: T-box transcription factor 19; Treg: Regulatory T; UMAP: Uniform manifold approximation and projection.

kinase/signal transducer and activator of transcription 3 (IL-6/JAK/STAT3) signaling pathways. In contrast, Tfh and proliferating T cells exhibited enrichment in fatty acid metabolism, apical junction regulation, and p53 signaling pathways [Figure 4H]. Moreover, scMetabolism was used to analyze the metabolic pathway activity of

tumor-infiltrating T cells. Proliferating T cells demonstrated markedly higher activity across many metabolic pathways compared to all other subsets. Treg cells were actively involved in arginine and proline metabolism, while Tfh cells were engaged in glycosphingolipid biosynthesis as well as glycine, serine, and threonine metabolism [Figure 4I].

Cellular interactions within the TME of PitNETs

Given the inherent heterogeneity of TME, CellPhoneDB was employed to systematically deconvolve the intercellular communication networks among transcriptionally defined cell subsets. Ligand-receptor analysis revealed preferential interactions between MPs and $CD4^+$ T-cell subsets, particularly Treg and Tfh cells [Figure 5A–C]. Then, selected ligand–receptor pair analysis further indicated that both Treg and Tfh cells interacted with monocytes, macrophages, or microglial cells primarily through the CTLA4–CD86 or CD28–CD86 pathways. Additionally, Treg and Tfh cells interacted with CAF3 through the TIGHT–NECTIN2 pathway [Figure 5B and C].

Subsequently, mIHC staining was conducted on tumor tissues containing macrophages, microglial cells, Treg cells, Tfh cells, and CAF3 from PIT1-lineage PitNETs ($n = 3$) to validate and delineate the complex interactions among these subsets [Figure 5D]. The mIHC results revealed a correlation between $CD68^+$ macrophages or microglial cells and $FOXP3^+$ Treg cells, as well as an association between $POSTN^+$ CAFs and $ICOS^+$ Tfh cells. These interactions suggested a potential modulation of tumor immune responses. To mechanistically validate the regulatory role of the CTLA4–CD86 pathway in Treg enriched PitNET microenvironments, *in vitro* coculture experiments were performed using $CD86^+$ macrophages and naive $CD4^+$ T cells. Flow cytometry results demonstrated that treatment with an anti-CD86 neutralizing antibody significantly attenuated Treg differentiation mediated by $CD86^+$ macrophages ($P < 0.01$) [Figure 5E and F]. This functional evidence identified CD86 as a pivotal node within the immunosuppressive cellular network, wherein macrophage-derived CD86 interacted with CTLA4 on infiltrating lymphocytes to promote Treg polarization.

Discussion

PitNETs often display significant heterogeneity in biological behavior, which complicates the diagnostic and treatment approaches.[5,37,38] This challenge is particularly acute for aggressive tumor subtypes, where conventional therapies often show limited effectiveness.[5] These factors underscore the urgent need for a deeper understanding of the lineage-specific TME and immune cell infiltration patterns in PitNETs.

In antitumor therapy, many previous studies have focused on targeting the tumor cells.[39–44] However, CAFs, as critical non-tumor components of the TME, can remodel the stromal architecture by secreting growth factors, inflammatory ligands, and ECM proteins, thereby driving tumor proliferation, conferring therapeutic resistance, and promoting immune evasion.[45] Furthermore, CAFs exhibit substantial molecular heterogeneity, with individual subsets displaying unique functional profiles.[46,47] This heterogeneity necessitates the development of subset-specific antitumor strategies.[48] Yet, despite this therapeutic significance, CAF heterogeneity across distinct PitNET lineages remains inadequately characterized. Here, we identified five functional CAF subsets associated with different biological processes. Notably, CAF3 demonstrated the highest abundance in PIT1 lineage PitNETs and exhibited marked enrichment in TGF-β signaling, ECM remodeling, and epithelial-mesenchymal transition pathways. In contrast, CAF5, which predominated in the TPIT lineage, showed involvement in pro-inflammatory responses. These subsets are similar to the previously described collagen-producing and inflammatory CAF subtypes, respectively.[49,50] Therefore, the proportions and distinct functions of CAF3 and CAF5 may reflect underlying heterogeneity in the TME of PitNETs.

The myeloid cell composition and functional states are critically involved in regulating tumor progression and metastasis.[51,52] Our analysis identified the presence of proliferating MPs, macrophages, monocytes, cDC1, cDC2, microglial cells, and pDCs in PitNETs. The proportions of monocytes and microglial cells varied across distinct PitNET lineages, whereas the macrophage proportions remained comparable across these lineages. Within the TME, macrophages undergo polarization into either M1 macrophages, which exhibit antitumor functions, or M2 macrophages, which support pro-tumor activities.[53] However, macrophage polarization is more complex than the M1/M2 binary classification, and its polarization process is highly dynamic and regulated by diverse microenvironmental signals.[54] Recent scRNA-seq studies of PitNETs have further identified distinct TAM transcriptional subtypes with unique functional states.[9,10] A population of microglial cells_CX3CR1 was observed, representing a terminally differentiated macrophage state. The developmental trajectory analysis demonstrated that these microglial cells_CX3CR1 and macrophages_CXCL3 originate from a shared Macrophages_C1QB precursor. Further analysis suggested that the differentiation of these cells is potentially regulated by IL6ST, NFKBIA, and TRA2B. Functionally, myeloid-derived suppressor cells exhibiting high CX3CR1 expression may facilitate tumor immune evasion and are correlated with poor clinical outcomes.[55,56]

Neutrophils infiltrate tumor tissues and dynamically modulate the TME.[57,58] However, their functional roles in PitNETs remain inadequately defined. Our findings indicated that there were eight distinct subsets within PitNETs, each with unique biological functions. Notably, Neutrophils_SPP1 were predominantly localized to the PIT1 lineage and correlated with shorter OS in the brain tumor cohort. This finding is consistent with previous reports indicating that high SPP1 expression is associated with poor prognosis across multiple cancer types. Moreover, SPP1, known as secreted phosphoprotein 1 and commonly referred to as osteopontin, has been shown to promote immune escape by mediating myeloid cell differentiation

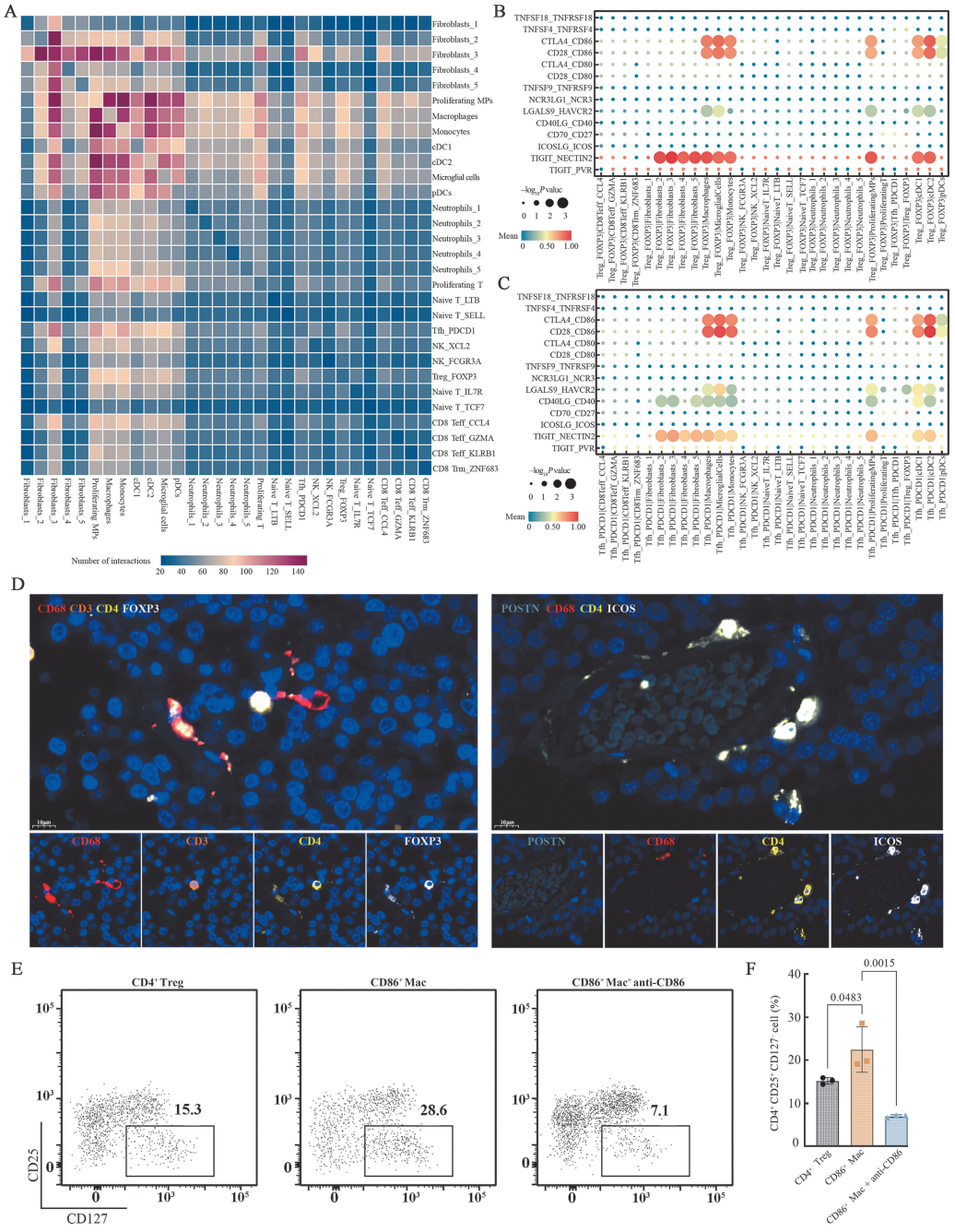

Figure 5: The cellular interactions within the TME of PitNETs. (A) Heatmap showing the total number of interactions among different cell types in PitNETs with CellPhoneDB analysis. (B, C) Ligand-receptor pair analysis using CellPhoneDB reveals distinct intercellular communication involving both Tregs (B) and Tfh (C) cells. *P*-values are indicated by circle size; scale is shown below the plot. The means of the average expression levels are indicated by color. (D) Representative mIHC staining shows colocalization of macrophages with CD4+ FOXP3+ Treg cells (red represents CD68+ macrophages and microglia; orange, yellow, and white represent Treg cells), as well as an association between POSTN+ CAFs and CD4+ ICOS+ Tfh cells (cyan represents CAFs; red represents macrophages; yellow and white represent Tfh cells) in PIT1 lineage PitNETs ($n = 3$). Scale bar as indicated. (E, F) Flow cytometry analysis of the proportion of Treg cells in different groups. Treg cell: CD4+ CD25+ CD127-. Three independent experiments. CAF: Cancer-associated fibroblast; CD: Cluster of differentiation; cDC: Conventional dendritic cell; CTLA4: Cytotoxic T-lymphocyte antigen 4; FOXP3: Forkhead box protein P3; HAVCR2: Hepatitis A virus cellular receptor 2; ICOS: Inducible T-cell costimulator; ICOSLG: Inducible COStimulator ligand; LGALS9: Lectin galactoside-binding soluble 9; Mac: Macrophage; mIHC: Multiplex immunohistochemistry; MP: Mononuclear phagocyte; NCR3: Natural cytotoxicity triggering teceptor 3; NCR3LG1: Natural cytotoxicity triggering receptor 3 ligand 1; NECTIN2: Nectin 2; pDC: Plasmacytoid dendritic cell; PDCD1: Programmed cell death protein 1; PIT1: Pituitary-specific transcription factor 1; PitNETs: Pituitary neuroendocrine tumors; POSTN: Periostin; PVR: Poliovirus receptor; Tfh: T follicular helper; TIGIT: T cell immunoreceptor with Ig and ITIM domains; TME: Tumor microenvironment; TNFSF: Tumor necrosis factor superfamily; Treg: Regulatory T.

and facilitating leukocyte migration.[59] However, further investigation is warranted to elucidate the precise mechanisms by which SPP1 neutrophil subset can regulate PitNET progression, which will guide the development of targeted therapies against this specific subset.

Although T cells play pivotal roles in antitumor immunity,[60] the distribution and phenotypic characteristics of T-cell subsets within PitNET lineages have not been completely elucidated. Our flow cytometry and mIHC analyses revealed a significantly elevated abundance of

Treg and Tfh cells within the PIT1 lineage. Furthermore, Treg cells exhibited significant upregulation of the IL6/JAK/STAT3 signaling pathway and actively drove arginine/proline metabolism. Previous work has suggested that activation of the STAT3 pathway can introduce immunosuppression within the TME. The underlying mechanisms involve the suppression of cytotoxic T lymphocyte activity and/or the enhancement of Treg recruitment.[61–64]

In the complex TME, dynamic interactions among cellular constituents are critically involved in driving tumor progression and immune modulation.[65,66] Therefore, this study further investigated the intercellular communication networks among diverse cell populations in the PitNET TME. Our research revealed distinct communication networks that included Treg and Tfh cells interacting with macrophages, microglia, and CAF3 in PitNETs via specific ligand-receptor pairs such as CTLA4-CD86, CD28-CD86, and T cell immunoreceptor with Ig and ITIM domains (TIGIT)-nectin 2 (NECTIN2). These results suggested a potential mechanism for immune-mediated modulation of PitNET development. Subsequent mIHC assays confirmed Treg-macrophage/microglia colocalization, indicating myeloid-mediated maintenance of Treg cells within the TME. In addition, prior research has well established that CAFs can influence T cell activities and functions in various cancers.[18,67] Consequently, the present investigation was specifically focused on CD86 interactions with Treg cells. *In vitro* coculture assays demonstrated that macrophage-derived CD86 could engage with CTLA4 on lymphocytes to drive Treg polarization, establishing CD86 as a key regulator in the immunosuppressive network. Previous reports have demonstrated that ICIs, including PD1 and CTLA4 inhibitors, have been used in the treatment of several aggressive PitNET cases.[68–71] However, because of the limited efficacy and these drugs' risk of adverse effects[5], personalized immunotherapy using immune classification offers a promising alternative.[72–73] Our study revealed significant immune cell composition heterogeneity among the distinct lineage-specific subtypes, further supporting the necessity of personalized treatment strategies for PitNETs. Moreover, our findings also highlight the CTLA4–CD86 axis as a potentially valuable therapeutic target. Further preclinical and large-scale clinical studies with long-term follow-up are still needed to confirm its effectiveness and identify biomarkers for response and prognosis.

Our current analysis has several limitations. First, the small sample size led to insufficient representation within each cell lineage subtype, affecting the statistical power and generalizability of the findings. Second, this study focused exclusively on tumor samples without including normal pituitary tissues as controls, which may have limited the ability to distinguish between tumor-specific and normal immune compositions. Third, highly abundant heterogeneous neutrophil populations were observed across the three PitNET lineages. Their precise function, whether promoting tumor growth or regression, requires further investigation at the single-cell level to be uncovered. Therefore, future studies should expand the sample size and include normal tissue controls to ensure the robustness and generalizability of the single-cell findings.

In summary, this study provides a comprehensive analysis of tumor-infiltrating immune cells in PitNETs, with a focus on immune heterogeneity and intercellular communication networks. Specifically, PIT1 lineage PitNETs exhibited an enrichment of Treg and Tfh cells, along with collagen-producing CAF3. Moreover, the CTLA4–CD86 pathway mediated a novel immunosuppressive interaction between Treg cells and macrophages, demonstrating its role in TME modulation and potential as a therapeutic target. These findings deepen our understanding of the PitNET immune complexity and provide translational insights for novel treatment development and immunotherapy research.

Data availability statement

The datasets generated and analyzed during this study are available from the corresponding author upon reasonable request.

Acknowledgments

The authors extend their heartfelt gratitude to Professor J.X.Z. and Z.C.L. from the Center for Applied Statistics at the School of Statistics, Renmin University of China, for their expert statistical consultation.

Funding

This study was supported by grants from the Nonprofit Central Research Institute Fund of Chinese Academy of Medical Sciences (No. 2022-JKCS-06), Capital Clinical Characteristic Diagnosis and Treatment Technology Research and Transformation Application (No. Z221100007422041), and Beijing Natural Science Foundation-Changping Innovation Joint Fund (No. L244030).

Conflicts of interest

None.

References

1. Melmed S. Pituitary-tumor endocrinopathies. N Engl J Med 2020;382:937–950. doi: 10.1056/NEJMra1810772.
2. Gittleman H, Ostrom QT, Farah PD, Ondracek A, Chen Y, Wolinsky Y, *et al*. Descriptive epidemiology of pituitary tumors in the United States, 2004-2009. J Neurosurg 2014;121:527–535. doi: 10.3171/2014.5.JNS131819.
3. Asa SL, Mete O, Perry A, Osamura RY. Overview of the 2022 WHO classification of pituitary tumors. Endocr Pathol 2022;33:6–26. doi: 10.1007/s12022-022-09703-7.
4. Melmed S, Kaiser UB, Lopes MB, Bertherat J, Syro LV, Raverot G, *et al*. Clinical biology of the pituitary adenoma. Endocr Rev 2022;43:1003–1037. doi: 10.1210/endrev/bnac010.
5. Raverot G, Ilie MD, Lasolle H, Amodru V, Trouillas J, Castinetti F, *et al*. Aggressive pituitary tumours and pituitary carcinomas. Nat Rev Endocrinol 2021;17:671–684. doi: 10.1038/s41574-021-00550-w.
6. Ilie MD, Vasiljevic A, Raverot G, Bertolino P. The microenvironment of pituitary tumors-biological and therapeutic implications. Cancers 2019;11:1605. doi: 10.3390/cancers11101605.
7. Marques P, Grossman AB, Korbonits M. The tumour microenvironment of pituitary neuroendocrine tumours. Front Neuroendocrinol 2020;58:100852. doi: 10.1016/j.yfrne.2020.100852.
8. Cui Y, Li C, Jiang Z, Zhang S, Li Q, Liu X, *et al*. Single-cell transcriptome and genome analyses of pituitary neuroendocrine

tumors. Neuro Oncol 2021;23:1859–1871. doi: 10.1093/neuonc/noab102.
9. Yan N, Xie W, Wang D, Fang Q, Guo J, Chen Y, *et al*. Single-cell transcriptomic analysis reveals tumor cell heterogeneity and immune microenvironment features of pituitary neuroendocrine tumors. Genome Med 2024;16:2. doi: 10.1186/s13073-023-01267-3.
10. Lin S, Dai Y, Han C, Han T, Zhao L, Wu R, *et al*. Single-cell transcriptomics reveal distinct immune-infiltrating phenotypes and macrophage-tumor interaction axes among different lineages of pituitary neuroendocrine tumors. Genome Med 2024;16:60. doi: 10.1186/s13073-024-01325-4.
11. Lyu L, Jiang Y, Ma W, Li H, Liu X, Li L, *et al*. Single-cell sequencing of PIT1-positive pituitary adenoma highlights the pro-tumour microenvironment mediated by IFN-gamma-induced tumour-associated fibroblasts remodelling. Br J Cancer 2023;128:1117–1133. doi: 10.1038/s41416-022-02126-5.
12. Chhabra Y, Weeraratna AT. Fibroblasts in cancer: Unity in heterogeneity. Cell 2023;186:1580–1609. doi: 10.1016/j.cell.2023.03.016.
13. Xu J, Liu C, Wu X, Ma J. Current immune therapeutic strategies in advanced or metastatic non-small cell lung cancer. Chin Med J 2023;136:1765–1782. doi: 10.1097/CM9.0000000000002536.
14. Guo X, Chang M, Li W, Qian Z, Guo H, Xie C, *et al*. Immune atlas of pituitary neuroendocrine tumors highlights endocrine-driven immune signature and therapeutic implication. Cell Rep 2025;44:115584. doi: 10.1016/j.celrep.2025.115584.
15. Paijens ST, Vledder A, de Bruyn M, Nijman HW. Tumor-infiltrating lymphocytes in the immunotherapy era. Cell Mol Immunol 2021;18:842–859. doi: 10.1038/s41423-020-00565-9.
16. Dai C, Liang S, Sun B, Kang J. The progress of immunotherapy in refractory pituitary adenomas and pituitary carcinomas. Front Endocrinol 2020;11:608422. doi: 10.3389/fendo.2020.608422.
17. De Leo A, Ugolini A, Yu X, Scirocchi F, Scocozza D, Peixoto B, *et al*. Glucose-driven histone lactylation promotes the immunosuppressive activity of monocyte-derived macrophages in glioblastoma. Immunity 2024;57:1105–1123.e8. doi: 10.1016/j.immuni.2024.04.006.
18. Mao X, Xu J, Wang W, Liang C, Hua J, Liu J, *et al*. Crosstalk between cancer-associated fibroblasts and immune cells in the tumor microenvironment: New findings and future perspectives. Mol Cancer 2021;20:131. doi: 10.1186/s12943-021-01428-1.
19. Moore J, Ma L, Lazar AA, Barcellos-Hoff MH. Mammary tumor-derived transplants as breast cancer models to evaluate tumor-immune interactions and therapeutic responses. Cancer Res 2022;82:365–376. doi: 10.1158/0008-5472.CAN-21-0253.
20. Liu X, Kong Y, Qian Y, Guo H, Zhao L, Wang H, *et al*. Spatial heterogeneity of infiltrating immune cells in the tumor microenvironment of non-small cell lung cancer. Transl Oncol 2024;50:102143. doi: 10.1016/j.tranon.2024.102143.
21. Micko A, Oberndorfer J, Weninger WJ, Vila G, Hoftberger R, Wolfsberger S, *et al*. Challenging Knosp high-grade pituitary adenomas. J Neurosurg 2019;132:1739–1746. doi: 10.3171/2019.3.JNS19367.
22. Xiao Y, Wang Z, Zhao M, Deng Y, Yang M, Su G, *et al*. Single-cell transcriptomics revealed subtype-specific tumor immune microenvironments in human glioblastomas. Front Immunol 2022;13:914236. doi: 10.3389/fimmu.2022.914236.
23. McGinnis CS, Murrow LM, Gartner ZJ. DoubletFinder: Doublet detection in single-cell RNA sequencing data using artificial nearest neighbors. Cell Syst 2019;8:329–337.e4. doi: 10.1016/j.cels.2019.03.003.
24. Vento-Tormo R, Efremova M, Botting RA, Turco MY, Vento-Tormo M, Meyer KB, *et al*. Single-cell reconstruction of the early maternal-fetal interface in humans. Nature 2018;563:347–353. doi: 10.1038/s41586-018-0698-6.
25. Wu Y, Yang S, Ma J, Chen Z, Song G, Rao D, *et al*. Spatiotemporal immune landscape of colorectal cancer liver metastasis at single-cell level. Cancer Discov 2022;12:134–153. doi: 10.1158/2159-8290.CD-21-0316.
26. Bergen V, Lange M, Peidli S, Wolf FA, Theis FJ. Generalizing RNA velocity to transient cell states through dynamical modeling. Nat Biotechnol 2020;38:1408–1414. doi: 10.1038/s41587-020-0591-3.
27. Wolf FA, Hamey FK, Plass M, Solana J, Dahlin JS, Gottgens B, *et al*. PAGA: Graph abstraction reconciles clustering with trajectory inference through a topology preserving map of single cells. Genome Biol 2019;20:59. doi: 10.1186/s13059-019-1663-x.
28. Tang Z, Kang B, Li C, Chen T, Zhang Z. GEPIA2: An enhanced web server for large-scale expression profiling and interactive analysis. Nucleic Acids Res 2019;47:W556–W560. doi: 10.1093/nar/gkz430.
29. Rebuffet L, Melsen JE, Escaliere B, Basurto-Lozada D, Bhandoola A, Bjorkstrom NK, *et al*. High-dimensional single-cell analysis of human natural killer cell heterogeneity. Nat Immunol 2024;25:1474–1488. doi: 10.1038/s41590-024-01883-0.
30. Hanzelmann S, Castelo R, Guinney J. GSVA: Gene set variation analysis for microarray and RNA-seq data. BMC Bioinformatics 2013;14:7. doi: 10.1186/1471-2105-14-7.
31. Kanehisa M, Goto S. KEGG: Kyoto encyclopedia of genes and genomes. Nucleic Acids Res 2000;28:27–30. doi: 10.1093/nar/28.1.27.
32. Liberzon A, Birger C, Thorvaldsdottir H, Ghandi M, Mesirov JP, Tamayo P. The Molecular Signatures Database (MSigDB) hallmark gene set collection. Cell Syst 2015;1:417–425. doi: 10.1016/j.cels.2015.12.004.
33. Ashburner M, Ball CA, Blake JA, Botstein D, Butler H, Cherry JM, *et al*. Gene ontology: Tool for the unification of biology. The Gene Ontology Consortium. Nat Genet 2000;25:25–29. doi: 10.1038/75556.
34. Zhou Y, Zhou B, Pache L, Chang M, Khodabakhshi AH, Tanaseichuk O, *et al*. Metascape provides a biologist-oriented resource for the analysis of systems-level datasets. Nat Commun 2019;10:1523. doi: 10.1038/s41467-019-09234-6.
35. Sekiya T, Yoshimura A. In vitro Th differentiation protocol. Methods Mol Biol 2016;1344:183–191. doi: 10.1007/978-1-4939-2966-5_10.
36. Tang H, Wang X, Bie Z, Yang Z, Wang B, Li S, *et al*. Pituitary adenomas with multiple cell lineage combinations: Clinicopathological features and short-term prognosis. J Neurosurg 2023;139:810–821. doi: 10.3171/2022.12.JNS222118.
37. Tatsi C, Stratakis CA. Aggressive pituitary tumors in the young and elderly. Rev Endocr Metab Disord 2020;21:213–223. doi: 10.1007/s11154-019-09534-8.
38. Raverot G, Burman P, McCormack A, Heaney A, Petersenn S, Popovic V, *et al*. European Society of Endocrinology Clinical Practice Guidelines for the management of aggressive pituitary tumours and carcinomas. Eur J Endocrinol 2018;178:G1–G24. doi: 10.1530/Eje-17-0796.
39. Lasolle H, Cortet C, Castinetti F, Cloix L, Caron P, Delemer B, *et al*. Temozolomide treatment can improve overall survival in aggressive pituitary tumors and pituitary carcinomas. Eur J Endocrinol 2017;176:769–777. doi: 10.1530/EJE-16-0979.
40. Elbelt U, Schlaffer SM, Buchfelder M, Knappe UJ, Vila G, Micko A, *et al*. Efficacy of temozolomide therapy in patients with aggressive pituitary adenomas and carcinomas-A German survey. J Clin Endocrinol Metab 2020;105:dgz211. doi: 10.1210/clinem/dgz211.
41. Gatto F, Arvigo M, Ferone D. Somatostatin receptor expression and patients' response to targeted medical treatment in pituitary tumors: Evidences and controversies. J Endocrinol Invest 2020;43:1543–1553. doi: 10.1007/s40618-020-01335-0.
42. Hewedi IH, Osman WM, El Mahdy MM. Differential expression of cyclin D1 in human pituitary tumors: Relation to MIB-1 and p27/Kip1 labeling indices. J Egypt Natl Canc Inst 2011;23:171–179. doi: 10.1016/j.jnci.2011.11.003.
43. Ben-Shlomo A, Cooper O. Role of tyrosine kinase inhibitors in the treatment of pituitary tumours: From bench to bedside. Curr Opin Endocrinol Diabetes Obes 2017;24:301–305. doi: 10.1097/MED.0000000000000344.
44. Jordan S, Lidhar K, Korbonits M, Lowe DG, Grossman AB. Cyclin D and cyclin E expression in normal and adenomatous pituitary. Eur J Endocrinol 2000;143:R1–R6. doi: 10.1530/eje.0.143r001.
45. Biffi G, Tuveson DA. Diversity and biology of cancer-associated fibroblasts. Physiol Rev 2021;101:147–176. doi: 10.1152/physrev.00048.2019.
46. Zhang H, Yue X, Chen Z, Liu C, Wu W, Zhang N, *et al*. Define cancer-associated fibroblasts (CAFs) in the tumor microenvironment: New opportunities in cancer immunotherapy and advances in clinical trials. Mol Cancer 2023;22:159. doi: 10.1186/s12943-023-01860-5.
47. Zhang F, Ma Y, Li D, Wei J, Chen K, Zhang E, *et al*. Cancer associated fibroblasts and metabolic reprogramming: Unraveling the intricate crosstalk in tumor evolution. J Hematol Oncol 2024;17:80. doi: 10.1186/s13045-024-01600-2.

48. Chen Y, McAndrews KM, Kalluri R. Clinical and therapeutic relevance of cancer-associated fibroblasts. Nat Rev Clin Oncol 2021;18:792–804. doi: 10.1038/s41571-021-00546-5.
49. Cords L, Engler S, Haberecker M, Ruschoff JH, Moch H, de Souza N, *et al*. Cancer-associated fibroblast phenotypes are associated with patient outcome in non-small cell lung cancer. Cancer Cell 2024;42:396–412e395. doi: 10.1016/j.ccell.2023.12.021.
50. Ma C, Yang C, Peng A, Sun T, Ji X, Mi J, *et al*. Pan-cancer spatially resolved single-cell analysis reveals the crosstalk between cancer-associated fibroblasts and tumor microenvironment. Mol Cancer 2023;22:170. doi: 10.1186/s12943-023-01876-x.
51. Barry ST, Gabrilovich DI, Sansom OJ, Campbell AD, Morton JP. Therapeutic targeting of tumour myeloid cells. Nat Rev Cancer 2023;23:216–237. doi: 10.1038/s41568-022-00546-2.
52. van Vlerken-Ysla L, Tyurina YY, Kagan VE, Gabrilovich DI. Functional states of myeloid cells in cancer. Cancer Cell 2023;41:490–504. doi: 10.1016/j.ccell.2023.02.009.
53. Mantovani A, Allavena P, Marchesi F, Garlanda C. Macrophages as tools and targets in cancer therapy. Nat Rev Drug Discov 2022;21:799–820. doi: 10.1038/s41573-022-00520-5.
54. Boutilier AJ, Elsawa SF. Macrophage polarization states in the tumor microenvironment. Int J Mol Sci 2021;22:6995. doi: 10.3390/ijms22136995.
55. Chaudhri A, Bu X, Wang Y, Gomez M, Torchia JA, Hua P, *et al*. The CX3CL1-CX3CR1 chemokine axis can contribute to tumor immune evasion and blockade with a novel CX3CR1 monoclonal antibody enhances response to anti-PD-1 immunotherapy. Front Immunol 2023;14:1237715. doi: 10.3389/fimmu.2023.1237715.
56. Jeong JM, Choi SE, Shim YR, Kim HH, Lee YS, Yang K, *et al*. CX3CR1 + macrophages interact with HSCs to promote HCC through CD8 + T-cell suppression. Hepatology 2024;82:655–668. doi: 10.1097/HEP.0000000000001021.
57. Giese MA, Hind LE, Huttenlocher A. Neutrophil plasticity in the tumor microenvironment. Blood 2019;133:2159–2167. doi: 10.1182/blood-2018-11-844548.
58. Que H, Fu Q, Lan T, Tian X, Wei X. Tumor-associated neutrophils and neutrophil-targeted cancer therapies. Biochim Biophys Acta Rev Cancer 2022;1877:188762. doi: 10.1016/j.bbcan.2022.188762.
59. Liu Y, Ye G, Dong B, Huang L, Zhang C, Sheng Y, *et al*. A pan-cancer analysis of the oncogenic role of secreted phosphoprotein 1 (SPP1) in human cancers. Ann Transl Med 2022;10:279. doi: 10.21037/atm-22-829.
60. Zeng Z, Chew HY, Cruz JG, Leggatt GR, Wells JW. Investigating T cell immunity in cancer: Achievements and prospects. Int J Mol Sci 2021;22:2907. doi: 10.3390/ijms22062907.
61. Fu W, Hou X, Dong L, Hou W. Roles of STAT3 in the pathogenesis and treatment of glioblastoma. Front Cell Dev Biol 2023;11:1098482. doi: 10.3389/fcell.2023.1098482.
62. Kitamura H, Ohno Y, Toyoshima Y, Ohtake J, Homma S, Kawamura H, *et al*. Interleukin-6/STAT3 signaling as a promising target to improve the efficacy of cancer immunotherapy. Cancer Sci 2017;108:1947–1952. doi: 10.1111/cas.13332.
63. Zou S, Tong Q, Liu B, Huang W, Tian Y, Fu X. Targeting STAT3 in cancer immunotherapy. Mol Cancer 2020;19:145. doi: 10.1186/s12943-020-01258-7.
64. Priceman SJ, Shen S, Wang L, Deng J, Yue C, Kujawski M, *et al*. S1PR1 is crucial for accumulation of regulatory T cells in tumors via STAT3. Cell Rep 2014;6:992–999. doi: 10.1016/j.celrep.2014.02.016.
65. Khosravi GR, Mostafavi S, Bastan S, Ebrahimi N, Gharibvand RS, Eskandari N. Immunologic tumor microenvironment modulators for turning cold tumors hot. Cancer Commun 2024;44:521–553. doi: 10.1002/cac2.12539.
66. Rahal Z, El Darzi R, Moghaddam SJ, Cascone T, Kadara H. Tumour and microenvironment crosstalk in NSCLC progression and response to therapy. Nat Rev Clin Oncol 2025;22:463–482. doi: 10.1038/s41571-025-01021-1.
67. Varveri A, Papadopoulou M, Papadovasilakis Z, Compeer EB, Legaki AI, Delis A, *et al*. Immunological synapse formation between T regulatory cells and cancer-associated fibroblasts promotes tumour development. Nat Commun 2024;15:4988. doi: 10.1038/s41467-024-49282-1.
68. Duhamel C, Ilie MD, Salle H, Nassouri AS, Gaillard S, Deluche E, *et al*. Immunotherapy in corticotroph and lactotroph aggressive tumors and carcinomas: Two case reports and a review of the literature. J Pers Med 2020;10:88. doi: 10.3390/jpm10030088.
69. Lamb LS, Sim HW, McCormack AI. Case report: A case of pituitary carcinoma treated with sequential dual immunotherapy and vascular endothelial growth factor inhibition therapy. Front Endocrinol 2020;11:576027. doi: 10.3389/fendo.2020.576027.
70. Sol B, de Filette JMK, Awada G, Raeymaeckers S, Aspeslagh S, Andreescu CE, *et al*. Immune checkpoint inhibitor therapy for ACTH-secreting pituitary carcinoma: A new emerging treatment? Eur J Endocrinol 2021;184:K1–K5. doi: 10.1530/EJE-20-0151.
71. Majd N, Waguespack SG, Janku F, Fu S, Penas-Prado M, Xu M, *et al*. Efficacy of pembrolizumab in patients with pituitary carcinoma: Report of four cases from a phase II study. J Immunother Cancer 2020;8:e001532. doi: 10.1136/jitc-2020-001532.
72. Fu C, Zhai Y, Yan L, Jin S, Shang J, Shi X, Wu D. Redefining multiple myeloma treatment: Advances, challenges, and future directions in immunotherapy. Chin Med J 2025;138:2399–410. doi: 10.1097/CM9.0000000000003655.
73. Xie N, Shen G, Huang C, Zhu H. Neoantigen-driven personalized tumor therapy: An update from discovery to clinical application. Chin Med J 2025;138:2057–2090. doi: 10.1097/CM9.0000000000003708.

How to cite this article: Zhang Z, Su H, Yin J, He JH, Hu YN, Li P, Liu PN. Single-cell transcriptomics reveals the landscape of immune phenotypes in pituitary neuroendocrine tumors. Chin Med J 2026;139:597–609. doi: 10.1097/CM9.0000000000003918